PERFORMANCE OF DOUBLE-T PRESTRESSED CONCRETE BEAMS STRENGTHENED WITH STEEL REINFORCED POLYMER

Paolo Casadei[1], Antonio Nanni[2], Tarek Alkhrdaji[3] and Jay Thomas[4]

ABSTRACT

In the fall of 2002, a two-storey parking garage in Bloomington, Indiana, built with precast prestrestressed concrete (PC) double-T beams, was decommissioned due to a need for increased parking-space. This led to the opportunity of investigating the flexural performance of the PC double-T beams, upgraded in the positive moment region with steel reinforced polymer (SRP) composite materials, representing the first case study where this material has been applied in the field. SRP makes use of high-strength steel cords embedded in an epoxy resin. This paper reports on the test results to failure of three beams: a control specimen, a beam strengthened with one ply of SRP and a third beam strengthened with two plies of SRP anchored at both ends with SRP U-wraps. Results showed that SRP can significantly improve both flexural capacity and enhance pseudo-ductility. Preliminary analytical work shows that the same approach used for externally bonded fiber reinforced polymer (FRP) can be satisfactorly used for SRP.

Keywords: double-T beams; ductility; flexure; in-situ load test; prestressed concrete; steel reinforced polymer; strengthening.

[1] Lecturer of Structural Engineering, Department of Architecture and Civil Engineering, University of Bath, Bath, BA2 7AY, United Kingdom
Tel. +44 1225 386748, Fax -386691, Email: P.Casadei@bath.ac.uk
[2] V & M Jones Professor, Department of Civil, Architectural and Environmental Engineering
223 Engineering Research Lab, University of Missouri-Rolla, Rolla, MO-65401 USA
[3] Structural Engineer, Strengthening Division of the Structural Group.
[4] Vice President, Structural Preservation Systems Inc.

1 INTRODUCTION

The use of advanced composite materials in the construction industry is nowdays a mainstream technology (Rizkalla and Nanni 2003), supported by design guidelines such as the ACI 440.2R-02 (2002) in the United States and the Fib-Bullettin 14 (2001) in Europe. Fiber reinforced polymer (FRP) composite materials, even though very attractive, may be hindered by lack of ductility and fire resistance. Both issues are currently under study by the research community (Williams et al. 2004, Bisby et al. 2004, Seible et al. 1997), in order to provide on one hand, better knowledge in terms of overall structural performance and, on the other, remedies such as coatings that could prolong fire resistance.

A new family of composite materials based on high strength twisted steel wires (about *7 times* stronger than typical common reinforcing bars) of fine diameter (*0.20~0.35 mm* (*0.0079~0.0138 in*) see Figure 1), that can be impregnated with thermo-set or cementitious resin systems is presented in this paper (Hardwire 2002). SRP has the potential to address the two shortcomings mentioned for FRP, in fact: a) steel cords have some inherent ductility; and b) impregnation with cementitious paste may overcome the problems of fire endurance.

The steel cords used in SRP are identical to those used for making the reinforcement of automotive tires, and manufactured to obtain the shape of the fabric tape prior to impregnation (Hardwire, 2002). The twisting of the wires allows some mechanical interlock between the cords and the matrix, and may also induce an overall ductile behavior upon stretching. Characterization work is currently in progress as necessary for implementation in future design guidelines.

Limited research results have been published on this new generation of composite materials. Huang et al. (2004) investigated the mechanical properties of SRP, testing different kinds of matrices, epoxy resin and cementitious grout, including a comparison between theoretical and experimental results needed for design. Test results showed that the material does not experience a substantial yielding, but rather a similar behavior to the one experienced by high-strength steel used in prestressed concrete (PC) construction, with a slightly non-linear range prior to rupture of the cords.

The opportunity for experimenting this new material in the field, became available in the winter of 2003 when the City of Bloomington, Indiana, decommissioned an existing parking garage near the downtown area, built with double-T PC beams. The concrete repair contractor, Structural Preservation Systems, Hanover, MD, strengthened in flexure the bottom stem of several double-T beams with with epoxy-based SRP. This paper reports on the experimental as well as analytical results of tests to failure conducted on three beams: a control specimen, a beam strengthened with one ply of SRP and a third beam strengthened with two plies of SRP anchored at both ends with U-wraps.

2 EXPERIMENTAL PROGRAM

2.1 Building Characteristics

The parking garage used for the tests was a two storey structure constructed in the 1980s (see Figure 3). It consisted of a reinforced concrete (RC) frame, cast in place columns and precast reversed-T PC beams, supporting double-T PC beams, of span length varying from *4.66 m* (*15.3 ft*) to *13.41 m* (*44 ft*).

Since no maintenance or construction records were available for the materials and the layout of the prestressing tendons, a field investigation was carried out. Based on the survey, it was determined that the double-T PC beams were of type 8DT32 according to the Prestressed Concrete Institute (1999) specifications (see Figure 4) with concrete topping of *76 mm* (*3in*), and with an arrangement of the tendons different from current specifications. For the span of *4.66 m* (*15.3 ft*), two straight 7-wire strands were found in each stem, each with a diameter of *12.7 mm* (*0.5 in*), corresponding to an area of *112* mm^2 (*0.174* in^2), the first at *248 mm* (*9.75 in*) from the bottom of the stem and the second spaced *305 mm* (*1 ft*) from the first one (see Figure 4). No mild reinforcement was found at any location. Welded pockets, connecting two adjacent beams, were positioned every *910 mm* (*3ft*) at a depth of *76 mm* (*3 in*) from top surface. Concrete properties were evaluated using three cores taken from three different beams at the location of the stem and an avarage concrete cylinder strength of f_c'*=34* N/mm^2 *(*f_c'*=5000 psi)* was found and its modulus of elasticity was determined according to ACI 318-02 Section 8.5.1 provisions (see Table 1). The strands properties were assumed to be conventional *1861 MPa* (*270 ksi*) strength and summarized in Table 1.

2.2 Specimens and Installation of Steel Reinforced Polymer

A total of three double-T PC beams were tested (see Figure 5): beam DT-C is the control beam, beam DT-1 represents the beam strengthened with one ply of SRP and DT-2U the one strengthened with 2 plies of SRP anchored with SRP U-wraps.

The epoxy resin for both strengthened beams was *SikaDur Resin 330*. Table 2 reports the resin properties supplied by the manufacturer and verified by testing according to ASTM standards by Huang et al. (2004). Figure 6*a* shows the mixing prior to installation. The choice of the resin was based on constructability so that it could be rolled

onto the surface for overhead applications, while having enough consistency, even before curing, to be able to hold the weight of the steel tape during cure. The tape was medium density consisting of *6.3 cords per cm* (*12 WPI*), with material properties defined in Table 3 (Huang et al. 2004). The typical stress-strain diagram for an impregnated medium density tape, tested following the ASTM D 3039 recommendations, is reported in Figure 2 (properties based on steel net area).

SRP was installed following the reccomendations of ACI 440.2R-02 (ACI 440) provisions for FRP materials. The sequence of installation steps is reported in Figure 6. The bottom stem of the double-T beams was first abrasive-blasted to ensure proper bonding of the SRP system. With the surface roughened and cleaned, the first layer of epoxy was directly applied (see Figure 6*b*), without primer coating. The steel tape was cut to length of *4.57 m* (*15 ft*) and width of *102 mm* (*4 in*), covering the bottom of the stem length and width entirely. A rib-roller was then utilized to press onto the tape to ensure epoxy impregnation and encapsulation of each cord and allow excess resin to be squeezed out. The excess resin was spread with a putty-knife to create an even surface (see Figure 6*c*) and a synthetic scrim was applied to avoid any dripping of the resin (see Figure 6*d*). For the two ply application, once the first ply was in place and the excess resin leveled, the second ply was installed, following an identical procedure. This time the ply started *152 mm* (*6 in*) away from the terminations of the first ply, making it *4.27 m* (*14 ft*) long. To provide a mechanical ancorage for the two longitudinal plies, an SRP U-wrap *914 mm* (*3 ft*) wide was installed at both ends of the stems (see Figure 6*e*). Due to the stiffness of the steel tape, pre-forming is done with a standard sheet metal bender before installation. For this reason, the U-wrap was obtained by overlapping two L-shaped wraps.

2.3 Test Setup and Instrumentation

The experimental setup is shown in Figure 7*a* and Figure 7*b*. The beams were tested under simply supported conditions and subject to a single concentrated load spread over both stems at mid-span, that is, 3-point bending at mid-span (see Figure 7*c*).

All three tests were conducted using a close-loop load configuration, where no external reaction is required. The load was applied in cycles by one hydraulic jack of *890 kN* (*200 kip*) capacity connected to a hand-pump. The load was transferred to the PC beam in two points through one spreader steel beam (see Figure 7*b*). The reverse-T PC-Ledger beams, on which the double-T beam rests, supplied the reaction. As the hydraulic jack extended, it pulled on the high-strength steel bars, which lifted the reaction bailey-truss below. The reaction truss was built with three bailey-truss frames *6.09 m* (*20 ft*) long assembled as per manufacturer's specifications (Mabey Bridge and Shore, Baltimore, MD), and properly designed to carry the test load (see Figure 7*a*). Plywood was placed at each contact point to protect the concrete. The load was measured using a *890 kN* (*200 kip*) load cell placed on top of the jack (see Figure 7*c*). The preparation work consisted of drilling one hole of small diameter (*~50 mm* (*2 in*)) necessary for passing the high-strength steel bar through the flange of the double-T PC beam and isolating each test specimen from the adjacent beams originally joined by the welded-pockets.

An electronic data acquisition system (see Figure 8*a*) recorded data from four linear variable differential transducers (LVDTs) and two electrical strain-gages applied to the SRP in beams DT-1 and DT-2U. Two LVDTs were placed at mid-span (see Figure 8*b*), and the remaining two LVDTs, were placed under the reverse-T ledger beams to verify

potential support settlements. Strain gages were installed at mid-span on the bottom flange of the two strengthened double-T beams, directly onto the SRP material.

2.4 On-Site Safety

Safety procedures were adopted during the performance of the tests. The parking garage areas affected by each test were fenced and no one allowed within such areas. Shoring was provided and designed to carry the weight of the beam tested (multiplied by a *safety factor* equal to *2.0* to account for impact) and the additional weight of the testing equipment. Shoring was not in direct contact with the beam stems to allow unobstructed deflection.

3 RESULTS AND DISCUSSION

All beams failed in flexure and had a similar behavior up to the cracking load. Beam DT-C failed due to fracture of the lowest tendon. In beam DT-1, since the SRP ply was not mechanically anchored, failure was dictated by peeling off of the ply from each stem almost simultanuously. Beam DT-2U, strengthened with two anchored plies per stem, failed due to rupture of the lower tendon. Table 4 reports the test results.

In beam DT-C flexural cracks were concentrated in the mid-span region where the point load was applied. As soon as cracking occurred, since no mild reinforcement was present and tendons were placed far away from the bottom of the stem, cracks developed throughout the entire stem. In beams DT-1 and DT-2U a similar behavior occurred with the difference that the presence of the SRP allowed the formation of additional flexural cracks (see Figure 9). In beam DT-1 the SRP laminate started debonding at mid-span initiated by the widening of mid-span cracks (see Figure 9*a*) and then progressed towards the supports (see Figure 9*b*). Complete detachment of the

laminate occurred at one end of the beam with part of the concrete substrate attached to the laminate, denoting a good interface bond between the concrete and the SRP. In beam DT-2, SRP could not completely peel off due to the presence of U-wraps. Delamination propagated from mid-span towards the supports similarly to Beam DT-1, until rupture of the lower tendon occurred, which was immediately followed by SRP rupture exactly at the location where the SRP U-wrap started. No shear cracks were noted on any of the three beams.

Figure 10 through Figure 12 shows the Load-vs-mid-pan Deflection curves for all three beams. The capacities of beams DT-1 and DT-2U increased by approximately *12* and *26%* with respect to the control specimen DT-C.

Figure 13 and Figure 14 report the Load-vs-Mid-Span Strain responses for beams DT-1 and DT-2U. Two distinct phases, pre- and post-cracking, characterize the behavior of each specimen. Up to cracking there was practically no strain in the SRP. Past the cracking load, the presence of the SRP significantly affected performance.

Beam DT-C (see Figure 10) cracked at a considerably lower load (*250.8 kN* (*56.4 kip*)), with respect to the other two strengthened specimens. The occurrence of the first crack, at mid-span only, corresponds to the load drop in the Load-vs-Displacement plot. Upon unloading, the beam remained almost perfectly elastic, recovering almost all deflection. At the third loading cycle the lower strand suddenly fractured at a load of *344.3 kN* (*77.4 kip*).

For beams DT-1 and DT-2U the cracking load increased of approximately *23%* and *17%* with respect to DT-C (see Figure 11 and Figure 12). The lower cracking load for DT-2U may be explained by the fact that the beam had been previously repaired by means of epoxy injection.

Beam DT-1 reached the peak load of *387 kN* (*87 kip*) and held it constant with increasing deflection, while SRP progressively delaminated from mid-span towards the support. The strain profile reported in Figure 13 shows how the SRP was not engaged until cracking occurred and as soon as the first crack opened at mid-span, the SRP bridged the crack and strain suddenly increased to approximately *5500* $\mu\varepsilon$ (strain-gauge was placed at mid span where the first crack occurred). The maximum strain recorded in the steel tape (*12300* $\mu\varepsilon$), prior to complete peeling-off, shows how the material was well bonded to the concrete substrate. The ductility reported in the load-deflection curve, is the result of the slow peeling propagation rather than to yielding of the reinforcing steel tape itself. Figure 2 shows in fact an almost elastic behavior till rupture of the SRP laminate.

Past the cracking load (Figure 12), beam DT-2U behaved almost linearly, although with a lower stiffness, until it reached the load of *400 kN (90 kip)* then, stiffness decreased significantly till the peak load was reached. When the load of *434 kN (97.6 kip)* was reached, the lower tendon ruptured and a sudden drop in the load-deflection curve was recorded. The strain in the SRP material when the tendon ruptured was *6400* $\mu\varepsilon$. At this stage, once the lower tendon ruptured, the SRP laminate was completely debonded except for the region where anhoring was provided by the U-wraps. The test was continued untill suddenly the SRP laminate ruptured at *388 kN* (*87.2 kip*). The strain recorded in the SRP laminate at failure was 12000 $\mu\varepsilon$, similar to the values attained in beam DT-1.

4 ANALYTICAL APPROACH

The conventional analytical approach outlined in ACI 318-02 (2002) was used in conjunction with ACI 440.2R-02 (2002) provisions to compute the ultimate capacity of the beams without considering safety factors normally included in design.

The SRP behavior was approximated as illustrated in Figure 2 (Huang et al. 2004) and the values used for f_{fu_SRP}, ε_{fu_SRP}, and E_{SRP} are reported in Table 3.

The moment capacity M_n, inclusive of the SRP strengthening, can then be computed following ACI 440 provisions, using the appropriate equations to compute γ and β_1 (Todeschini et al. 1998) so that a rectangular stress block suitable for the particular level of strain in the concrete could be used, as (see also Figure 15):

$$M_{n\_SRP} = A_{pB} f_{pB} \left(d_{pB} - \frac{\beta_1 c}{2} \right) + A_{pT} f_{pT} \left(d_{pT} - \frac{\beta_1 c}{2} \right) + A_{SRP} f_{fe\_SRP} \left(h - \frac{\beta_1 c}{2} \right) \quad (1)$$

where the first two terms of the equation represent the existing prestress steel reinforcement, with the index *pB* and *pT* indicating the contribution of the bottom and top tendons, and assuming the following:

- total losses in the prestress tendons = *30%*
- in-place moment, prior to testing, only due to beam self weight .

The third term, of Eq.(1), represents the SRP contribution with the following assumptions being made:

- the area of SRP is computed as:

$$A_{SRP} = n\left(t_{SRP} \cdot w_{SRP}\right) \quad (2)$$

  where the n represents the number of plies, t_{SRP} the thickness of one ply (obtained by multiplying the area of one cord by the number of cords in the installed ply and dividing by the width of the ply) and w_{SRP} the width of the ply;

- the $k_{m,}$ bond reduction factor used to compute the effective stress in the SRP, has been computed according to ACI 440 provisions, using SI units, as follow:

$$\kappa_m = \frac{1}{60\varepsilon_{fu\_SRP}} \cdot \left(1 - \frac{nE_{SRP}t_{SRP}}{360,000}\right) \le 0.90 \qquad (3)$$

being $nE_{SRP}t_{SRP} \le 180,000$ for both beams DT-1 and DT-2U.

Table 5 reports on the analytical results. As reported in the second column, none of the tested beams reached the ultimate compression strain of ε_{cu}*=0.003*. Beam DT-C was found to fail in tension due to rupture of the lower tendon, as found experimentally, with a strain in the lower tendon of ε_{pB}*=0.023* and the ultimate failure load was found to be less than the experimental by only *2%*. Both Beam DT-1 and DT-2U were found to fail due to attainment of the effective SRP strain value, that were 0.0149 and 0.0139 for beams DT-1 and DT-2U respectively. Even though the experimental and analytical capacity values are very close, a convincing and exhaustive calibration of the k_m factor and the corresponding delamination need to be undertaken in order to validate these findings.

5 CONCLUSIONS

The following conclusions may be drawn from this experimental program:

- SRP composite materials have shown to be effective in increasing the flexural capacity of the double-T PC beams.
- End anchors in the form of SRP U-wraps have shown to be effective by preventing a complete detachment, once debonding has occurred throughout the concrete-SRP interface.

- SRP is similar to FRP in terms of ease of installation, although self weight should not be ignored when selecting the resin system in overhead applications.
- Epoxy resin behaved well in bonding the steel tape to the concrete substrate.
- The analytical validation, using ACI 440 provisions has proven to be effective in anticipating the ultimate capacity, although further investigation in a controlled laboratory environment is need to properly calibrate the bond factor k_m.

6 ACKNOWLEDGMENTS

This research study was sponsored by the National Science Foundation Industry/University Cooperative Research Center on Repair of Buildings and Bridges (RB^2C) at the University of Missouri – Rolla. Hardwire LLC., Pocomoke City, MD, provided the steel tapes and Sika Corporation, Lyndhurst, NJ, the resins for the installation. The City of Bloomington, IN, provided the opportunity for testing the structure.

REFERENCES

ACI 318-02, 2002: "Building Code Requirements for Structural Concrete and Commentary (318R-02)," Published by the American Concrete Institute, Farmington Hills, MI, pp. 443.

ACI 440.2R-02, 2002: "Guide for the Design and Construction of Externally Bonded FRP Systems for Strengthening Concrete Structures," Published by the American Concrete Institute, Farmington Hills, MI, pp. 45.

ASTM D 3039, 2002: "Test Method for Tensile Properties of Fiber Resin Composites" Published by the American Society for Testing and Materials, West Conshohocken, PA, pp. 13.

Bisby, L.A., Kodur, V.K.R., and Green, M.F. "Performance in Fire of FRP-Confined Reinforced Concrete Columns," Fourth International Conference on Advanced Composite Materials in Bridges and Structures - ACMBS-IV July 20-23, 2004 The Westin Hotel, Calgary, Alberta, Canada.

FIB Bullettin 14 (2001). "Design and use of externally bonded fibre reinforced polymer reinforcement (FRP EBR) for reinforced concrete structures, by 'EBR' working party of FIB TG 9.3, July 2001, 138 pp.

Hardwire LLC, 2002, "What is Hardwire," www.hardwirellc.com, Pocomoke City, MD.

Huang, X., Birman, V., Nanni, A., and Tunis, G., "Properties and potential for application of steel reinforced polymer and steel reinforced grout composites," Composites, Part B: Engineering, Volume 36, Issue 1, January 2004, Pages 73-82.

Mabey Bridge & Shore, Inc., www.mabey.com, Baltimore, MD.

Nawy, G. E., "Prestressed Concrete", Prentice Hall, Upper Saddle River, NJ, 2002, 789 pp.

PCI (1999): “PCI Design Handbook: Precast and Prestressed Concrete”, Published by the Precast/ Prestressed Concrete Institute, Chicago, IL.

Rizkalla, S. and Nanni, A. (2003) “Field Applications of FRP Reinforcement: Case Studies” ACI Special Publication 215, Published by the American Concrete Institute, Farmington Hills, MI.

Seible, F.; Priestley, M. J. N.; Hegemier, G. A.; and Innamorato, D., 1997, “Seismic Retrofit of RC Columns with Continuous Carbon Fiber Jackets,” Journal of Composites for Construction, No. 1, pp. 52-62.

Sika, 2004, “Sikadur 330”, www.sikausa.com, Lyndhurst, NJ.

Todeschini, C., Bianchini, A, and Kesler, C. (1982) "Behavior of Concrete Columns Reinforced with High Strength Steels." ACI Journal, Proceedings, Vol. 61, No. 6, pp 701-716, November-December

Williams, B.K., Kodur, V.K.R., Bisby, L.A., and Green, M.F. “The Performance of FRP-Strengthened Concrete Slabs in Fire,” Fourth International Conference on Advanced Composite Materials in Bridges and Structures - ACMBS-IV July 20-23, 2004 The Westin Hotel, Calgary, Alberta, Canada.

LIST OF TABLES

Table 1 - Properties of Construction Materials

Material	Cylinder Compressive Strength, MPa (psi)	Yield Strength MPa (ksi)	Rupture Strength MPa (ksi)	Elastic modulus[2] MPa (ksi)	7 wire Tendon Cross Section, Ap mm^2 (in^2)
Concrete [1]	34.4 (5,000)	-	-	27,600 (4,000)	-
Steel	-	1585 (230)	1862 (270)	200,000 (29,000)	112 (0.174)

[1] Average of 3 specimens [76.2 mm×152.4 mm (3 in×6 in) cylinders].

[2] $E_c = 4700\sqrt{f_c'}$ ACI 318 Section 8.5.1

Table 2 - Mechanical Properties of Epoxy Resin

Matrix	Tensile Strength, MPa (psi)	Ultimate Rupture Strain ε^*_{fu} (%)	Tensile Modulus of Elasticity, MPa (ksi)
SikaDur 330[1]	30 (4350)	1.5	3800 (551)

[1] Values provided by the manufacturer (Sika, 2004)

Table 3 - Material Properties of Steel Tape

Cord Coating	Cord Area per 12 Wires, mm^2 (in^2)	Cords per cm (in)	Nominal Thickness[1], t_{SRP} mm (in)	Tensile Strength f_{fu_SRP}, MPa (ksi)	Ultimate Rupture Strain ε_{fu_SRP} (mm/mm)	Tensile Modulus of Elasticity, GPa (ksi)
Brass	0.396 (0.000615)	3.7 (9.5)	0.148 (0.0058)	3070 (447)	0.0167	184 (26700)

[1] The nominal thickness has been computed assuming the area of each cord and counting the number of cords in each ply, reported in *cords per cm*

Table 4 – Beam Test Results

Beam	Failure load kN (kip)	Load Capacity Increase	SRP Strain at Failure ε_{SRP} ($\mu\varepsilon$)	Failure Mode
DT-C	344 (77.4)	1	-	Rupture of Lower Tendon
DT-1	387 (87)	1.12	12280	SRP Delamination
DT-2U	434 (97.6)	1.26	6400	Rupture of Lower Tendon

Table 5 – Analytical Beam Results at Ultimate

Beam	Concrete Strain ε_c	Neutral Axis Position c mm (in)	Effective Stress in the Tendons after Losses MPa (ksi)	Top Tendon Strain ε_{pB}	Bottom Tendon Strain ε_{pB}	κ_m Bond Factor	Existing Substrate Strain ε_{bi} [(1)]	SRP Strain ε_{SRP}	M_n kN-m (kip-ft)	P_u kN (kip)	Failure Mode	$P_{u\text{-Experimental}}$ / $P_{u\text{-Analytical}}$
DT-C	0.0010	21.08 (0.83)	1303 (189)	0.012	0.0230	N/A*	N/A*	N/A*	393 (290)	337 (75.8)	Attainment of Limit Tendon Strain	0.98
DT-1	0.0006	34.8 (1.37)		0.0053	0.0106	0.900	-0.0001	0.0149	454 (335)	389 (87.5)	Attainment of SRP Effective Strain Limit	1.00
DT-2U	0.0006	37.3 (1.47)		0.0049	0.0099	0.842		0.0139	513 (380)	442 (99.4)		1.02

*N/A = Not Applicable

(1)Determined from an elastic analysis considering only the self weight of the beams, at time of SRP installation

LIST OF FIGURES

a) Steel Cord with Wires Wrapped by One Wire

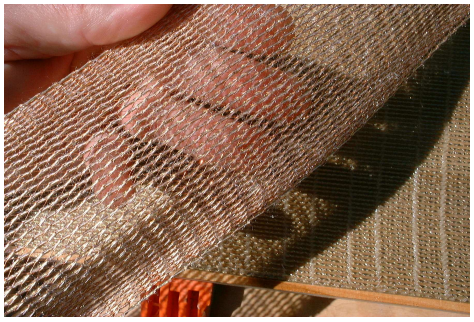

b) Tape with Cords Held Together by Polyester and Copper Knits

Figure 1 – Example of Steel Cord and Tape

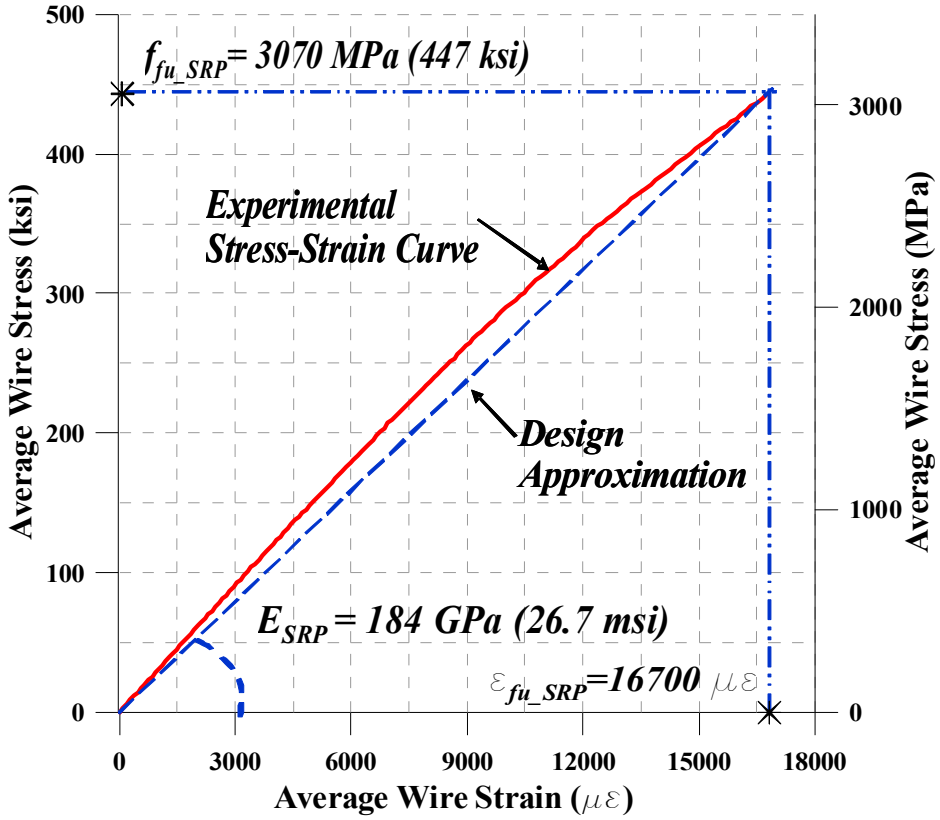

Figure 2 – SRP Laminate Stress vs Strain Behavior

a) Side View of Parking Garage

b) Top View of the Deck

c) Bottom View of the Deck

Figure 3 – Bloomington Parking Garage

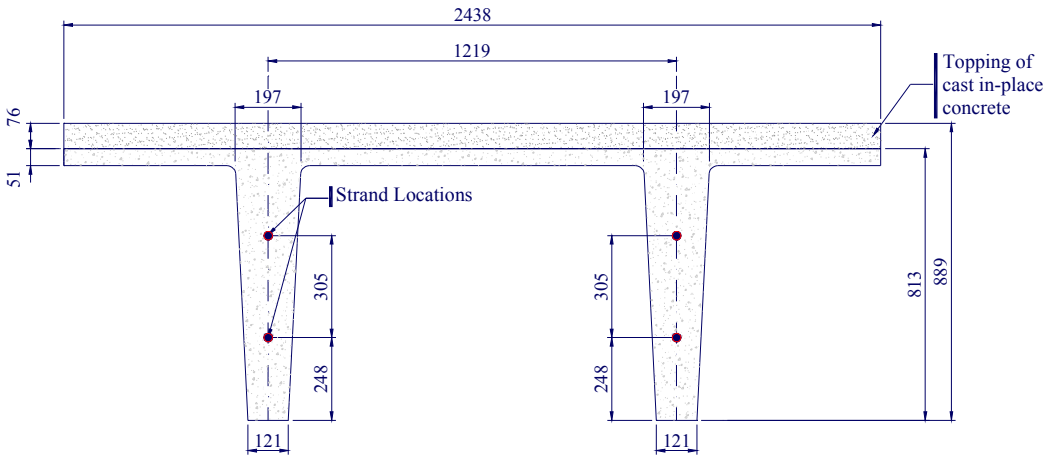

Figure 4 – Double-T Geometry Details (*SI units 1 mm = 0.039 in*)

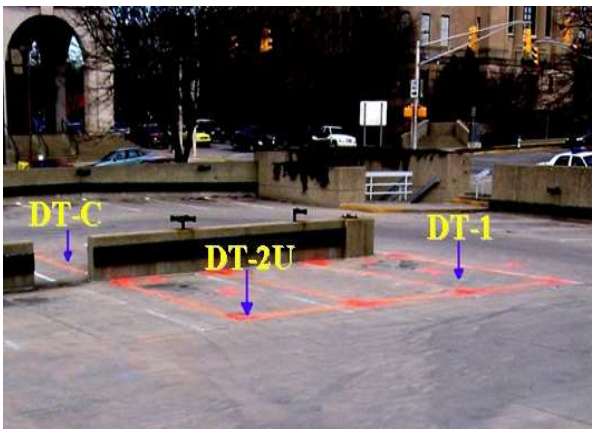

a) Saw-Cut Marks on Top of Deck

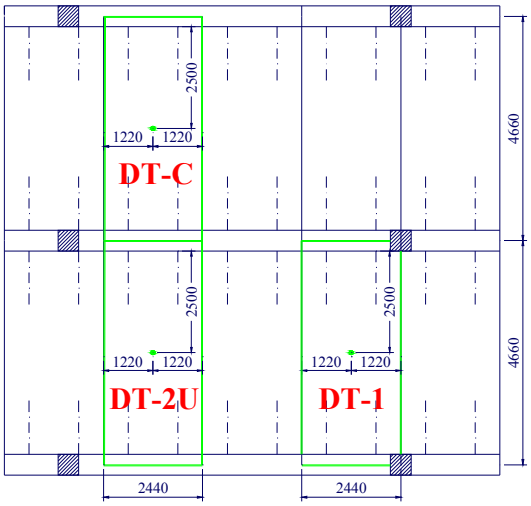

b) Plan View

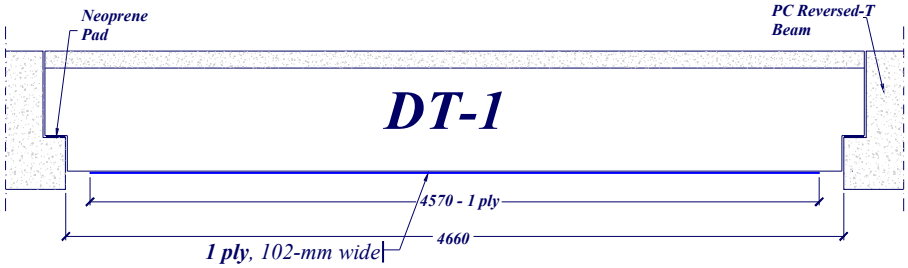

c) Beam Strengthened with 1 ply (DT-1)

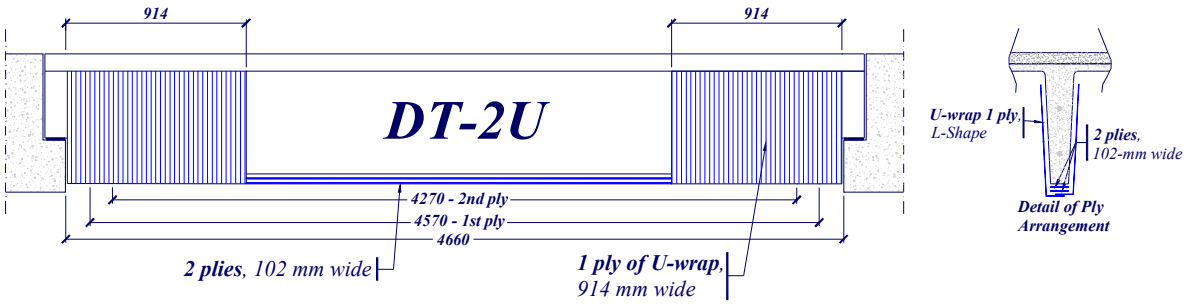

d) Beam Strengthened with 2 plies + U-wrap (DT-2U)

Figure 5 – Test Beams (*SI units 1 mm = 0.039 in*)

a) Mixing of the Epoxy Resin

b) Application of Longitudinal Ply

c) Squeezing Out the Resin Excess

d) Application of Scrim on Longitudinal Ply

e) Application of U-Wraps

f) Application of Epoxy on U-Wrap

Figure 6 – SRP Installation Procedure

a) Bottom View

b) Top View

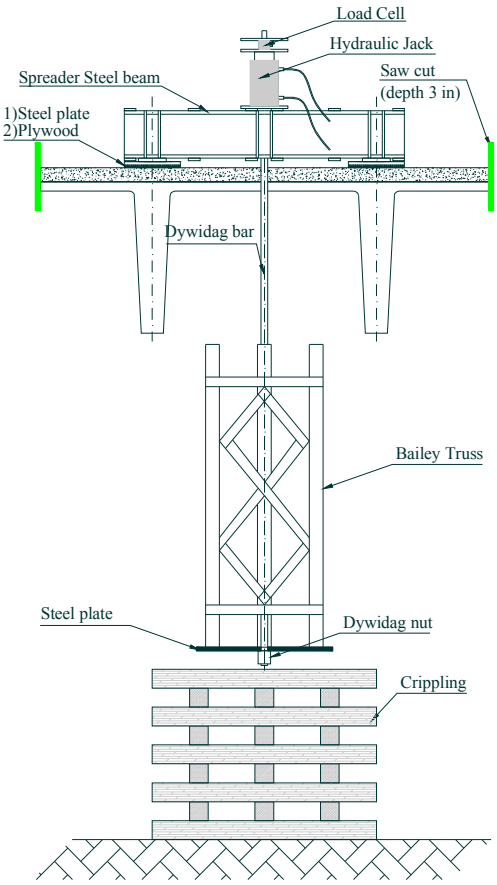

c) Cross Section at Mid-Span

Figure 7 – Test Set Up

a) Data Acquisition System

b) LVDT Locations

Figure 8 – Installed Instrumentation

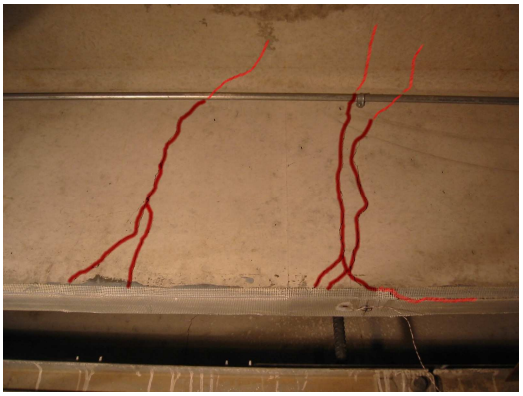

a) Crack Propagation Prior to Complete Peeling

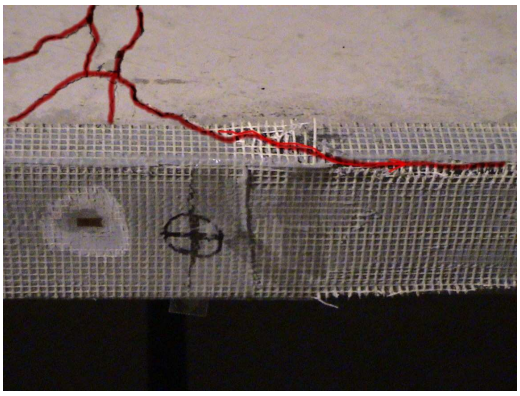

b) Debonding Propagation from Mid-Span

Beam DT-1

c) SRP Rupture

d) Rupture of the Lower Tendon

Beam DT-2U

Figure 9 – Failure Mechanisms in Strengthened Beams

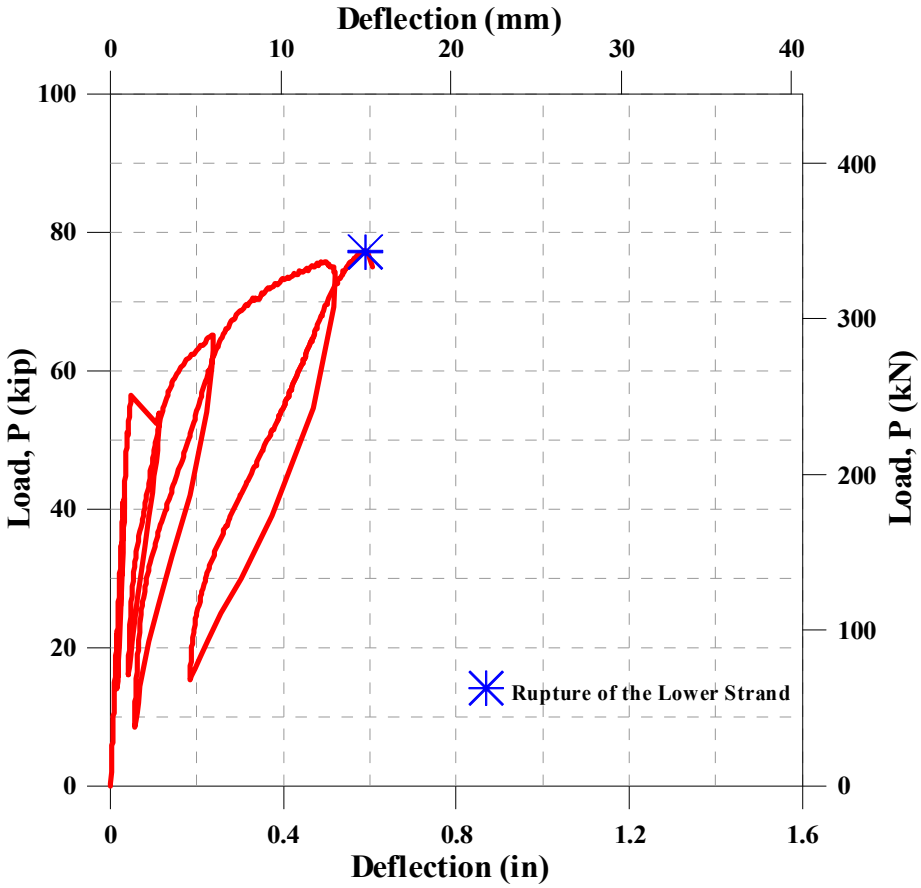

Figure 10 – Load vs Mid-Span Deflection (*Beam DT-C*)

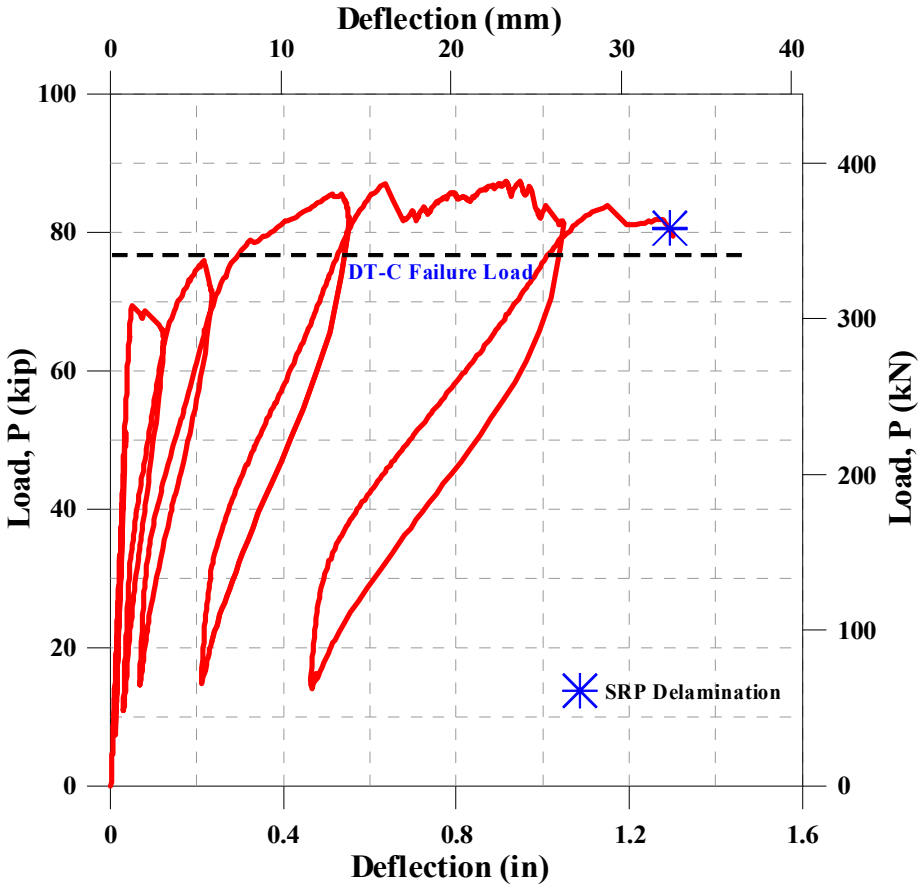

Figure 11 – Load vs Mid-Span Deflection (*Beam DT-1*)

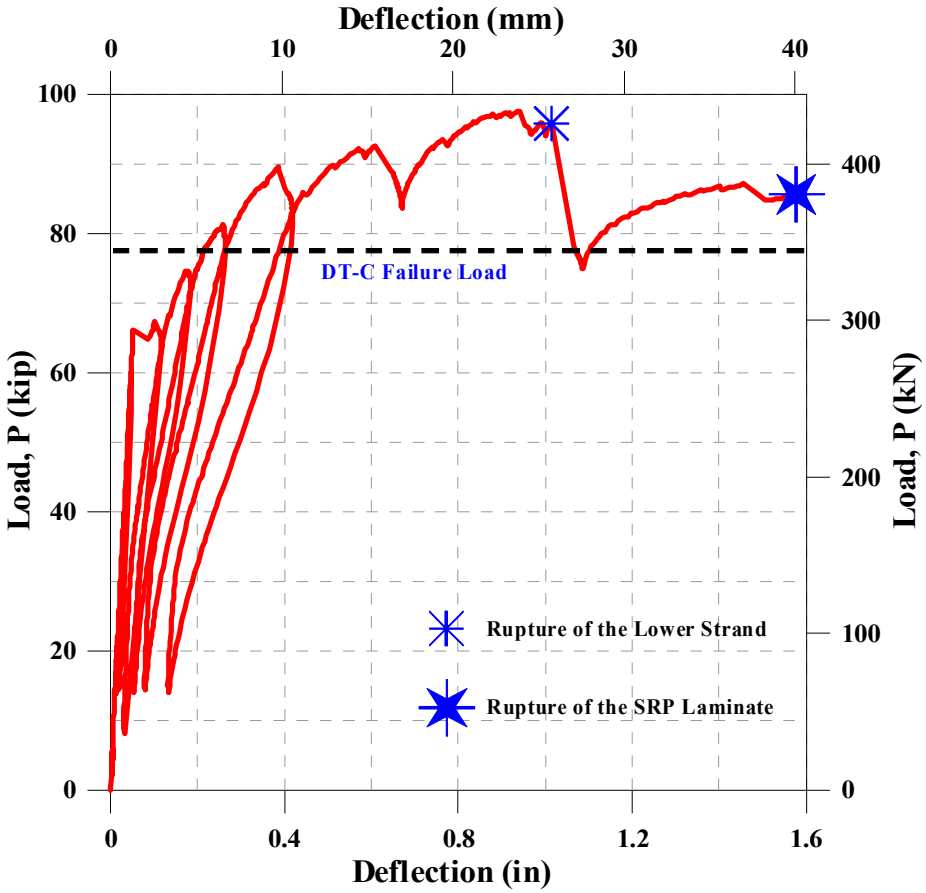

Figure 12 – Load vs Mid-Span Deflection (*Beam DT-2U*)

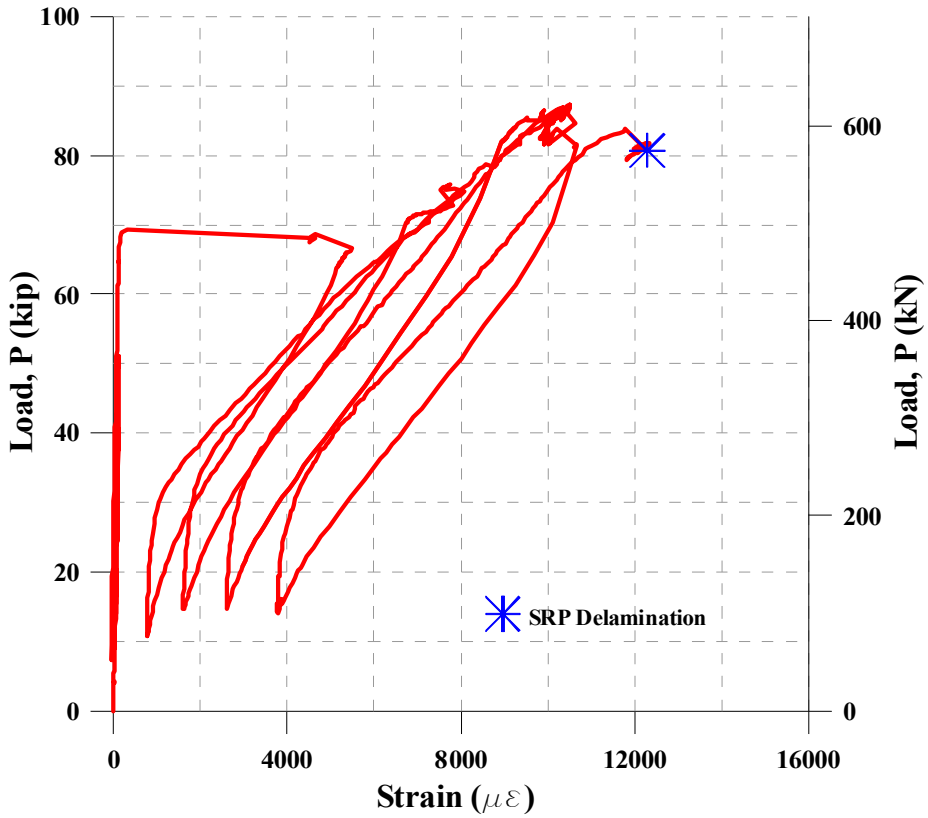

Figure 13 – Load vs Mid-Span Strain (*Beam DT-1*)

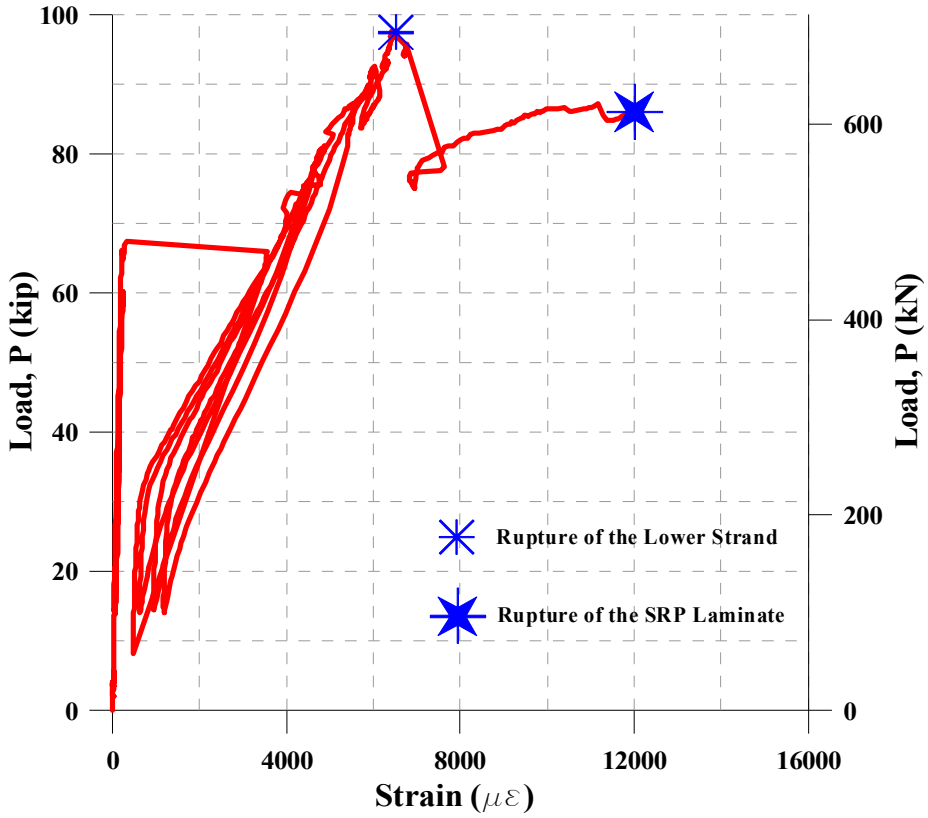

Figure 14 – Load vs Mid-Span Strain (*Beam DT-2U*)

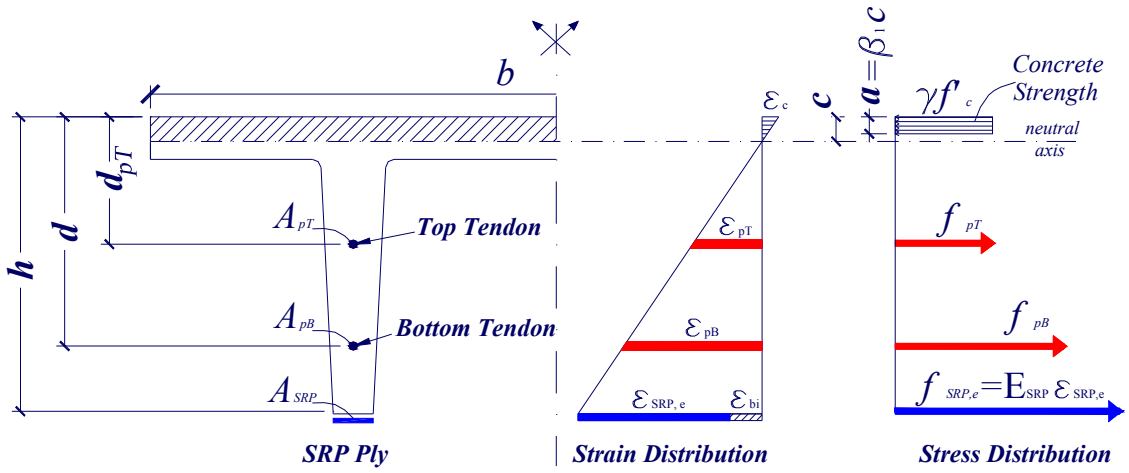

Figure 15 – Strain and Stress Distribution Across Beam Depth

NOTATION

A_{SRP} = $n(t_{SRP} w_{SRP})$ area of SRP reinforcement [mm^2]

A_{pB} = area of bottom steel tendon reinforcement [mm^2]

A_{pT} = area of top steel tendon reinforcement [mm^2]

c = depth of the neutral axis [mm]

E_{SRP} = $\frac{f_{fu\_SRP}}{\varepsilon_{fu\_SRP}}$ tensile modulus of elasticity of SRP [MPa]

E_c = $4700\sqrt{f_c'}$ tensile modulus of elasticity of concrete (ACI 318 Section 8.5.1) [MPa]

d_{pB} = depth of bottom steel tendon [mm]

d_{pT} = depth of top steel tendon [mm]

f_c' = ultimate compressive strength of concrete [MPa]

f_{fe_SRP} = effective stress in the SRP; stress level attained at section failure [MPa]

f_{fu_SRP} = $\overline{f_{fu\_SRP}} - 3\sigma$ ultimate design tensile strength in the SRP [MPa]

$\overline{f_{fu\_SRP}}$ mean ultimate tensile strength of SRP based upon a population of tests as per ASTM D 3039 [MPa]

f_{pB} = stress in bottom steel tendon at ultimate [MPa]

f_{pT} = stress in top steel tendon at ultimate [MPa]

h = height of the cross section [mm]

t_{SRP} = nominal thickness of one ply of SRP reinforcement [mm]

w_{SRP} = width of one ply of SRP [mm]

ε_c = strain level in the concrete [mm/mm]

ε_c' = $\frac{1.71 f_c'}{E_c}$ ultimate compressive strain of concrete (Todeschini et al. 1998) [mm/mm]

ε_{fu_SRP} = $\overline{\varepsilon_{fu\_SRP}} - 3\sigma$ design rupture strain in the SRP [mm/mm]

$\overline{\varepsilon_{fu\_SRP}}$ = mean rupture strain of SRP based upon a population of tests as per ASTM D 3039 [mm/mm]

β_1 = $2 - \frac{4\left[\left(\varepsilon_c/\varepsilon_c'\right) - \tan^{-1}\left(\varepsilon_c/\varepsilon_c'\right)\right]}{\left(\varepsilon_c/\varepsilon_c'\right)\ln\left(1+\varepsilon_c^2/\varepsilon_c'^2\right)}$ ratio of the depth of the equivalent rectangular stress block to the depth of the neutral axis (Todeschini et al. 1998)

γ = $\frac{0.9\ln\left(1+\frac{\varepsilon_c^{\,2}}{\varepsilon_c'^{\,2}}\right)}{\beta_1 \frac{\varepsilon_c}{\varepsilon_c'}}$ multiplier on f_c' to determine the intensity of an equivalent rectangular stress distribution for concrete (Todeschini et al. 1998)

k_m = Bond dependent coefficient for flexure